Results in Physics 51 (2023) 106700

Contents lists available at ScienceDirect

Results in Physics

journal homepage: www.elsevier.com/locate/rinp

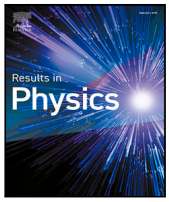

# Using advanced analysis together with fractional order derivative to investigate a smoking tobacco cancer model

Ismail Shah [a,*], Eiman [a], Hussam Alrabaiah [b,c,*], Burhanettin Ozdemir [d], Ateeq ur Rehman Irshad [d]

[a] Department of Mathematics, University of Malakand, Chakdara, Dir(L), 18000, KPK, Pakistan
[b] College of Engineering, Al Ain University, Al Ain, United Arab Emirates
[c] Department of Mathematics, Tafila Technical University, Tafila, Jordan
[d] Department of Mathematics and Sciences, Prince Sultan University, Riyadh 11586, Saudi Arabia

ARTICLE INFO

*Keywords:*
Strength number
Epidemiological modeling
Second derivative analysis
Tobacco cancer smoking model
Fractional order model

ABSTRACT

This research manuscript is devoted to investigate a smoking tobacco cancer model by applying some advanced techniques based on second derivative. The snuffing class is included in the construction of our model. The stability of the spread of the cancer disease due to tobacco is examined using the reproductive number concept. It is also advisable to look into the many scenarios in which the infectious classes might decline or vanish. Researchers calculated the reproductive number to create projections for the future. It hardly guarantees a thorough investigation, though. In light of this, the concept of strength number and the study of second derivatives for mathematical models are recommended using Laypunove functions to get more detailed information for future predictions. As a result, we investigate the proposed model using the second derivative technique to compute strengthen number. By calculating the aforesaid number, future proposals can be predicted. Finally, we make an effort to examine the proposed model under fractional order derivative to present some graphical simulations using different fractional order. In this regard, some numerical tools are utilized to approximate the proposed model for graphical investigations.

## Introduction

The use of tobacco dates back more than 4000 years. It was used by Native Americans as a narcotic drug. In 1493, Christopher Columbus returned it to Europe. Europe experienced a rapid growth of tobacco smoking during the 16th and 17th centuries. Annual tobacco consumption in the United States rose from 5 billion in 1905 to 17 and 90 billion in 1915 and 1925, respectively. As the harmful effects of tobacco became more widely known in the 1950s. Therefore in that time, anti-tobacco activities were launched. Around the same time, cigarette producers began producing filter cigarettes in an effort to reduce the negative effects of those campaigns. The 1970s is considered the introduction of lite cigarettes, which contained less nicotine and tar than filter cigarettes. In 1939, Muller published the pioneering research on the epidemiological association between smoking cigarettes and lung cancer (see [1]). After Muller's findings proved the cause-and-effect relationship between cigarette smoking and lung cancer in the 1950s, large case-control studies were carried out in the United States and Great Britain (we refer [2,3]). In 1964, a report published [4] which concluded that smoking cigarettes was the main contributing factor to lung cancer in men. In 1980, a similar partnership amongst women was also founded.

Lung cancer is the leading cause of cancer-related death worldwide. More than 160,000 fatalities from lung cancer have been reported in the US in 2007 and more than a million deaths from the disease worldwide. According to [5], smoking is the main risk factor for lung cancer. The body's immune system may get weakened by the poisons in cigarette smoke, making it more challenging to eradicate cancer cells. As a result, cancer cells continue to multiply. Smoke from cigarettes contains poisons that can alter or harm a cell's DNA. According to [6–8], smokers have a 30-fold increased risk of developing cancer than nonsmokers. According to estimates, one-third of people are smoking in most of the developed countries around the world. In addition, the number of women who smoke is also day by day increasing. One-third of all adult fatalities are expected to be caused directly by tobacco smoking by 2025, when 10 million deaths are expected. Large cohort studies have demonstrated the link between smoking and lung cancer [9,10]. Additionally, it is believed that smoking cigarettes accounts for between 70 and 80 percent of women's and

* Corresponding authors.
*E-mail addresses:* ismail8leu@gmail.com (I. Shah), ehuzaifa@gmail.com (Eiman), hussam.alrabaiah@aau.ac.ae (H. Alrabaiah), bozdemir@psu.edu.sa (B. Ozdemir), airshad@psu.edu.sa (A.u.R. Irshad).

https://doi.org/10.1016/j.rinp.2023.106700
Received 2 June 2023; Received in revised form 15 June 2023; Accepted 28 June 2023
Available online 4 July 2023

nearly 90 percent of men's chance of developing lung cancer. It is estimated that smoking causes about 90% of lung cancer fatalities. Compared to non-smokers, lifelong smokers have a 20–40 times increased risk of developing lung cancer. In the US, lung cancer is the cause of 26% and 31% of all cancer-related deaths in men and women, respectively. Overall, only 15% of people survive for five years, and only 42% do so for one year. Lung cancer claims more lives than prostate, breast, colon, and pancreatic cancers combined, we refer about the detail [11].

Woloshin and his co-authors have presented the health risks connected to smoking status in a fresh context. For males 60 years of age and older who smoke, the death rate from lung cancer is equal to the death rate from heart disease. After the age of 50, it is ten times more likely to die from prostate or colon cancer. For women who smoke, the risk of dying from lung cancer surpasses the chance of dying from breast cancer after the age of 40 [12]. Lung cancer and chronic obstructive pulmonary disease (COPD) are both made worse by a range of defective cells, cytokines, and growth factors that are produced as a result of smoking tobacco. Inflammation may encourage lung cancer in a variety of different ways. For instance, inflammatory cells' reactive nitrogen or oxygen species may bind to DNA and result in genetic alterations [13,14]. Patients who smoke after receiving cancer treatment face extra difficulties. Giving up smoking reduces the likelihood of developing recurring lung cancer and may increase the survival time of cancer patients. To save lives and reduce the risks associated with smoking, doctors should emphasize the benefits of quitting to both healthy individuals and cancer patients.

Here, it is remarkable that the technique of epidemiology is used to identify the root causes of diseases and other health issues in populations. In epidemiology, the population is the patient, and people are viewed as a whole. The said branch tremendously attracted the attention of researchers during last several decades. Different diseases have been modeled using various concepts of mathematics. Because, mathematical models are powerful tools increasingly used to describe real-world problems. For instance, we refer some applications of mathematical models as [15,16], and [17]. For recent work in epidemiology, we refer [18]. Numerous mathematical models for the transmission of the disease have been used to predict future patterns of spread with some effectiveness. The main objective is to comprehend the asymptotic spread so that measures can be implemented to combat and control viral infection and dissemination. To better comprehend these models, a number of mathematical ideas have been developed. Here, we refer some useful studies like [19–21].

During the modeling process, partial differential equations or ordinary differential equations have been used by mathematicians to transform the observable data into mathematical equations. In this regards, recently researchers have increasingly considered fractional order derivatives instead of traditional. Because the said operators with different kinds of kernels have the ability to model the real-world problems with more realistic way as compared to integer order. Some recent investigations are refereed here as [22–26]. The generated equation system, whether linear or nonlinear, is subjected to further investigation. In the preliminary study, equilibrium points (endemic and disease-free) were sought (see [27]). Following this analysis, a stability study that takes into account both global and asymptotic global stability is typically carried out to identify the circumstances under which the infectious classes will either increase, decrease, or remain constant (we refer [28,29]). If the spread will remain stable or not depends on the reproduction number, which can be computed in a variety of ways, such as by estimating the subsequent matrix generation. Finally, the study of the sign for the associated Lyapunov function's first derivative is undertaken to give a thorough grasp of the stability. Although thousands of articles have been written on the issue and similar analysis have been conducted, not much has changed since the concept of reproductive number was originally put forth. For some more details reader should read the work published in [29,30].

It has been noted that the fundamental reproduction number is insufficient for forecasting the future dynamics of detail transmission. As a result, some researchers have demonstrated that a different metric known as the strengthen number can aid in future prediction more. Additionally, the Lyapunov function's second derivative test might inform us of the specific transmission dynamics. In this study, we compute the second derivative test of the Lyapunov function and strengthen number for our suggested model which has been updated form of the model studied in [31] as

$$\begin{aligned}
\frac{dP}{dt} &= \Lambda - \frac{\beta_1}{N}\log(PI_L+1) + \delta_1 T + \delta_2^* C - \mu P,\\
\frac{dI_L}{dt} &= \frac{\beta_1}{N}\log(PI_L+1) - \beta_2 I_L I_C - (\alpha_1+\delta_3+\gamma_1+\mu)I_L,\\
\frac{dI_C}{dt} &= \beta_2 I_L I_C - \alpha_2 I_C - (\gamma_2+\mu)I_C + \alpha_1 I_L,\\
\frac{dI}{dt} &= \alpha_2 I_C - (\alpha_3+\gamma_3-\mu)I,\\
\frac{dT}{dt} &= \delta_3 I_L - \delta_4 T - (\delta_1+\mu)T + \alpha_3 I - \delta_5 T,\\
\frac{dC}{dt} &= \delta_4 T - \delta_2^* C - \mu C,\\
\frac{dR}{dt} &= \delta_5 T - \mu R,
\end{aligned} \tag{1}$$

where $N(t)$ is the total size individuals in community at time $t$, i.e., $N(t) = P(t) + I_L(t) + I_C(t) + I(t) + T(t) + C(t) + R(t)$. Here to be noted that the variables and parameters in our proposed model are non-negative. We consider the following conditions for our proposed model (1)

$$\begin{aligned}
&P(0) = P^0 \geq 0,\ I_L(0) = I_L^0 \geq 0,\ I_C(0) = I_C^0 \geq 0,\ I(0) = I^0 \geq 0,\\
&T(0) = T^0 \geq 0,\ C(0) = C^0 \geq 0, R(0) = R^0 > 0.
\end{aligned} \tag{2}$$

In addition, the variable, parameters involve in our proposed model and their physical description is given in Table 1.

It is remarked that the flow chart of the model described in Fig. 1 for further better understanding. Additionally, it has recently been discovered that fractional calculus significantly and more sophisticatedly models the majority of real-world issues. According to studies, fractional-order models do better at describing memory in biological and epidemiological systems than conventional integral-order models. Therefore, in order to understand our proposed model, it is important to reformulate the previous model to the fractional order model. A significant amount of work has been done using the aforementioned notions. Citations for some commonly used works in this regard include [32–35], and [36]. Different varieties of fractional differential operators have recently been introduced. The aforementioned operators are increasingly being employed to look into various issues in the actual world. Some outstanding findings are cited as [37,38]. There are various advantages of fractional order operators over traditional classical order. For instance fractional differential operators have greater degree of freedom and they permit to describe a real world phenomenon with more sophisticated form. Another one is that long and short memory characteristics are also nicely explained by using the aforesaid area as compared to integer order. The models involve fractional derivatives with local or nonlocal kernels describe the results in global ways because

**Table 1**
Nomenclatures and their physical description of the model (1).

| Nomenclature | Description |
|---|---|
| $P(t)$ | The Susceptible class |
| $I_L(t)$ | The Latently infected class |
| $I_C(t)$ | The Chronically infected class without treatment |
| $I(t)$ | The Infectious class without treatment |
| $T(t)$ | The Infectious class with treatment |
| $C(t)$ | The Cancer infectious class |
| $R(t)$ | The Recovered population |
| $\Lambda$ | Population size |
| $\beta_1$ | Disease transmission coefficient from $I_L$ |
| $\beta_2$ | transmission coefficient from $I_L$ to $I_C$ |
| $\delta_1$ | Rate of transferring from $I$ to $T$ |
| $\delta_2^*$ | Rate of transferring of from $C$ to $P$ |
| $\delta_3$ | Fraction of TB infective that move from $I_L$ to $T$ class |
| $\delta_4$ | Fraction of TB infective that move from $T$ to $C$ class |
| $\delta_5$ | Fraction of TB infective that move from $T$ to $R$ class |
| $\mu$ | Death rate in all compartment |
| $\alpha_1$ | The Rate at which individual leave $I_L$ and enter to $I_C$ class |
| $\alpha_2$ | The transferring of individuals from $I_C$ to $I$ class |
| $\alpha_3$ | The Rate at which individual leave $I$ and enter to $T$ class |
| $\gamma_1,\ \gamma_2,\ \gamma_3$ | Disease induced death rate in $I_L,\ I_C,\ I$ respectively |

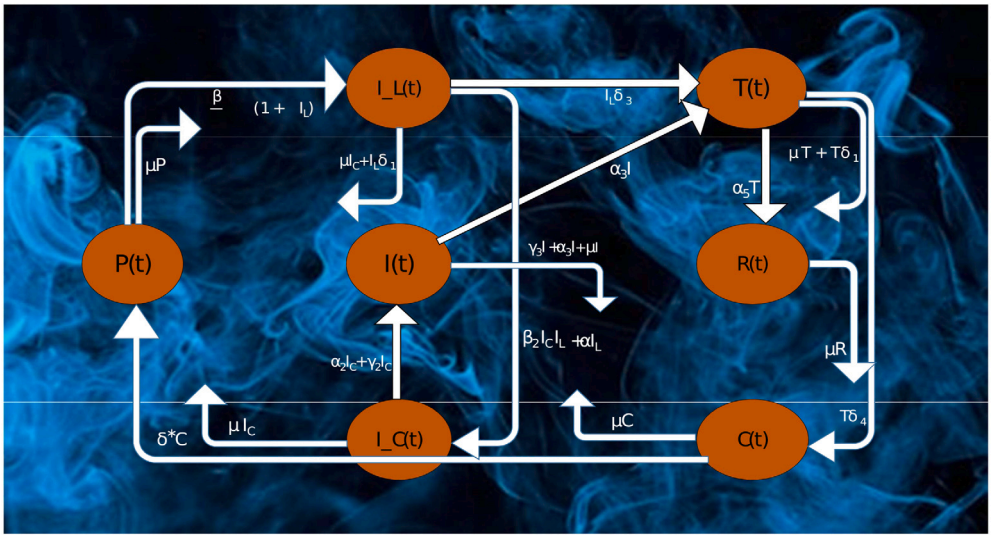


**Fig. 1.** Flow chart for our model (1).

such operators are global in nature, while intiger order are local in nature. The most significant features of fractional calculus is complete spectrum representation of a function to whom it applied which contains the corresponding integer counter part as a special case. We refer some usefulness of the said area in [39–41]. A popular topic of study at the moment is the study of biological models under fractional order derivatives. Fractional calculus is a powerful tool that researchers are employing to examine biological issues. For some important contributions, see [40,42–44]. The applicability of fractional calculus and its sibilance can be further studied in [44,45], and [46].

Here we state researchers have used various techniques to compute the basic thresholds number also called fundamental reproductive number. For instance authors [47] used procedure based on next-generation matrix to compute the basic reproduction number in ecological epidemiology model. In the same way other researchers have used various tools to calculate the aforementioned number, we refer [48–52]. Recently researchers have investigated that the said number cannot detect comprehensively about the future of a transmission dynamics. Therefore, they have introduced another quantity called strengthen number using the second derivative roles. The new number has the ability that it tells us about the future of a transmission dynamics in detailed way. Some real contribution in this regard, we refer as [53]. Also, the Lyapunov functions plays a vital role in constructive study on epidmology. Therefore recently, a survey of constructing Lyapunov functions for mathematical models in population biology has been investigated in [54]. For further frequent results [55]. We will also attempt to investigate our proposed model (1) under the concept of fractional order derivatives, which is inspired by the applications of fractional calculus. We will create a numerical program using the Euler technique to simulate the outcomes graphically for various fractional orders.

Organization of manuscript: The part first "Introduction" of the paper is devoted to a detailed introduction. The second portion "Preliminaries" is devoted to basic results. In addition, the part "Boundedness, Positivity of Solution, and Equilibrium Points" contains some fundamental results about the proposed model. Moreover Section "Main Results" contains main results which has some subsections further. Also, we present numerical results and simulations using traditional order model "Numerical Presentations and Discussion". The portion "Fractional Order Model and Numerical Simulations" contains fractional order model and its numerical investigations. Additionally, the paper is wind of with a brief conclusion in "Conclusion".

## Preliminaries

Here, we recollect some definitions which are needed for fractional part.

**Definition 1** ([46]). For a function $P : \mathcal{R}^+ \to \mathcal{R}$ and $\varrho \in (0, 1]$, the left Caputo fractional derivative of order $\varrho$ of the function $P$ is defined as

$$^{C}D_t^{\varrho} P(t) = \frac{1}{\Gamma(n-\varrho)} \int_0^t P^{(1)}(\varsigma)(t-\varsigma)^{-\varrho} d\varsigma.$$

In the same way, the corresponding Riemann–Liouville fractional integral associated with the power-law kernel is defined as

$$I_t^{\varrho} P(t) = \frac{1}{\Gamma(\varrho)} \int_0^t (t-\varsigma)^{\varrho-1} P(\varsigma) d\varsigma.$$

In addition, the given theorem is also important to convert fractional differential problem to fractional integral problem.

**Theorem 2** ([46]). *Let $P \in C[0, \tau]$, then the solution of the problem if $\Psi : [0, \tau] \times \mathcal{R}^+ \to \mathcal{R}$*

$$\begin{aligned} ^{C}D_t^{\varrho} P(t) &= \Psi(t, P(t)), \ \varrho \in (0, 1], \\ P(0) &= P_0 > 0 \end{aligned}$$

*is given by*

$$P(t) = P_0 + \int_0^t \frac{(t-\varsigma)^{\varrho-1}}{\Gamma(\varrho)} \Psi(\varsigma, P(\varsigma)) d\varsigma. \tag{3}$$

## Boundedness, positivity of solution, and equilibrium points

Find out the first derivative of $N(t)$ and using plugging the values from the model (1), we obtain

$$\frac{dN}{dt} = \Lambda - \mu N - \gamma_1 I_L + \alpha_1 I_C - \gamma_2 I_C - \gamma_3 I.$$

By under the concentration assumptions, the parameters and the variables are non-negative, so the last equation can simply rewrite as

$$\frac{dN}{dt} + \mu N \leq \Lambda.$$

One can reach to the solution with concern condition has the form

$$0 < N(t) \leq \frac{\Lambda}{\mu} + N(0) e^{-\mu t}. \tag{4}$$

The term $e^{-\mu t}$ tends to zero as time increases without bound. As how much time increases, (4) implies that the total population in community is bounded by $\frac{\Lambda}{\mu}$. From the above scenario, we claim the positively invariant biologically feasible region of proposed model has the form

$$\Omega = \left\{ \left(P, I_L, I_C, I, T, C, R\right) \in \mathcal{R}_+^7 \middle| 0 < N(t) \leq \frac{\Lambda}{\eta} \right\}.$$

Next, we deals with positivity of the solution of the proposed model under consideration. By picking the first equation of the model under consideration, which for all $t \geq 0$, has the form

$$\begin{aligned} \frac{dP}{dt} &= \Lambda - \frac{\beta_1}{N} \log(P I_L + 1) + \delta_1 T + \delta_2^* C - \mu P, \\ &\geq -\frac{\beta_1}{N} \log P - \mu P \\ &\geq -\frac{\beta_1}{N} (\sup_{t \in D_P} \log |P|) - \mu \sup_{t \in D_P} |P| \\ &\geq -\left[ \frac{\beta_1}{N} (\sup_{t \in D_P} |\log P| + \mu \sup_{t \in D_P} |P|) \right] \\ &\geq -\left[ \frac{\beta_1}{N} (\| \log P \|_\infty + \mu \| P \|_\infty) \right]. \end{aligned}$$

Integrating this subject to the initial conditions (2) has the form

$$P(t) \geq P^0 \exp^{-(\mu + \frac{\beta_1}{N})t} + \frac{\beta_1}{\mu N + \beta_1}, \text{ for all } t \geq 0.$$

Moving on the same line, one can verifies the positivity of the remaining solutions of the proposed system.

### *Disease-free equilibrium*

Initially we interest to determine the equilibrium states of the proposed model. The primary possible nontrivial condition of the given model is that when there is no contamination of the smoking disease in a the population. This state of the system called the disease free state. This state

is obtained by treating the infectious classes set to zero in the given model. It is straight forward to verify that the disease free state, $\mathcal{K}^0$, of model (1) is given by $\mathcal{K}^0 = (\Lambda/\mu, 0, 0, 0, 0)$. Since all classes other than the susceptible class are zero in this case, it turns out $N = S^0$. We derive endemic equilibrium points as

$$\begin{aligned}
\Lambda - \frac{\beta_1}{N}\log(PI_L+1) + \delta_1 T + \delta_2^* C - \mu P &= 0\\
\frac{\beta_1}{N}\log(PI_L+1) - \beta_2 I_L I_C - (\alpha_1+\delta_3+\gamma_1+\mu)I_L &= 0\\
\beta_2 I_L I_C - \alpha_2 I_C - (\gamma_2+\mu)I_C + \alpha_1 I_L &= 0\\
\alpha_2 I_C - (\alpha_3+\gamma_3-\mu)I, &= 0\\
\delta_3 I_L - \delta_4 T - (\delta_1-\mu)T + \alpha_3 I - \delta_5 T &= 0\\
\delta_4 T - \delta_2^* C - \mu C &= 0\\
\delta_5 T - \mu R &= 0.
\end{aligned} \tag{5}$$

Then the endemic equilibrium points are

$$\begin{aligned}
P^* &= \frac{-2\beta_1}{\mu N}\left(\frac{P^* {I_L}^* - 1}{P^* {I_L}^* + 1}\right) + \frac{R^*}{\delta_5}\left(\delta_1 + \frac{{\delta_2}^*}{{\delta_2}^* + \mu}\right)\\
{I_L}^* &= \frac{2\beta_1\zeta_1}{N\zeta_2\left(\alpha_1+\delta_3+\mu+\gamma_1+\beta_2{I_C}^*\right)}\\
{I_C}^* &= \frac{1}{\beta_2}\left(\frac{2\beta_1\zeta_1}{N\zeta_2 {I_L}^*} - \alpha_1 - \delta_3 - \mu - \gamma_1\right)\\
I^* &= \frac{\alpha_2 {I_L}^*\left(\alpha_1+\beta_2{I_C}^*\right)}{\left(\alpha_2+\gamma_2+\mu\right)\left(\alpha_3+\gamma_3-\mu\right)}\\
T^* &= \frac{{I_L}^*\left(\delta_3+\alpha_2\alpha_3\left(\alpha_1+\beta_2{I_C}^*\right)\right)}{\left(\alpha_2+\gamma_2+\mu\right)\left(\alpha_3+\gamma_3-\mu\right)\left(2\delta_4-\mu+\delta_5\right)}\\
R^* &= \frac{\delta_5 {I_L}^*\left(\delta_3+\alpha_2\alpha_3\left(\alpha_1+\beta_2{I_C}^*\right)\right)}{\mu\left(\alpha_2+\gamma_2+\mu\right)\left(\alpha_3+\gamma_3-\mu\right)\left(2\delta_4-\mu+\delta_5\right)}\\
C^* &= \frac{{I_L}^*\left(\delta_3+\alpha_2\alpha_3\left(\alpha_1+\beta_2{I_C}^*\right)\right)}{\left(\alpha_2+\gamma_2+\mu\right)\left(\alpha_3+\gamma_3-\mu\right)\left(2\delta_4-\mu+\delta_5\right)\left({\delta_2}^*+\mu\right)},
\end{aligned} \tag{6}$$

where

$$\begin{aligned}
\zeta_1 &= \frac{\alpha_2+\gamma_2+\mu}{\alpha_1+\beta_2{I_C}^*} - \frac{1}{P^*{I_C}^*},\\
\zeta_2 &= \frac{\alpha_2+\gamma_2+\mu}{\alpha_1+\beta_2{I_C}^*} + \frac{1}{P^*{I_C}^*}.
\end{aligned}$$

*Basic reproduction number*

Here, we discuss the stability of the possible equilibrium states of the proposed model. To start with, we consider it advantageous to determine the threshold quantity $\mathcal{R}_0$. For this purpose, we exploit the so-called next generation method [47]. To proceed further, we take into account the infectious classes in the proposed model and consider the following sub-system

$$\begin{aligned}
\frac{dI_L}{dt} &= \frac{\beta_1}{N}\log(PI_L+1) - \beta_2 I_L I_C - (\alpha_1+\delta_3+\gamma_1+\mu)I_L,\\
\frac{dI_C}{dt} &= \beta_2 I_L I_C - \alpha_2 I_C - (\gamma_2+\mu)I_C + \alpha_1 I_L,\\
\frac{dI}{dt} &= \alpha_2 I_C - (\alpha_3+\gamma_3-\mu)I,\\
\frac{dC}{dt} &= \delta_4 T - \delta_2^* C - \mu C.
\end{aligned} \tag{7}$$

Following, we find the necessary matrices for the computation of the threshold quantity. Matrices required for this situation are

$$F = \begin{bmatrix} \frac{\beta_1 P}{N(PI_L+1)} - \beta_2 I_C & -\beta_2 I_L & 0 & 0\\ \beta_2 I_C & \beta_2 I_L & 0 & 0\\ 0 & 0 & 0 & 0\\ 0 & 0 & 0 & 0 \end{bmatrix}, \text{ and } V = \begin{bmatrix} m_1 & 0 & 0 & 0\\ -\alpha_1 & m_2 & 0 & 0\\ 0 & -\alpha_2 & m_3 & 0\\ 0 & 0 & 0 & m_4 \end{bmatrix}.$$

where

$$m_1 = \alpha_1+\delta_3+\mu+\gamma_1, \quad m_2 = \alpha_2+\gamma_2+\mu, \quad m_3 = \gamma_3+\alpha_3-\mu,$$

and $m_4 = \mu + \delta_2^*$ under the fact $N = S^0$. The multiplicative inverse of the matrix $V$ has the form

$$V^{-1} = \begin{bmatrix} 1 & 0 & 0 & 0 \\ \frac{1}{m_1} & \frac{1}{\alpha_1} & 0 & 0 \\ \frac{\alpha_1\alpha_2}{m_1m_2} & \frac{\alpha_2}{m_2} & 1 & 0 \\ -\frac{\alpha_1\alpha_2}{m_1m_2} & -\frac{\alpha_2}{m_2} & -1 & 1 \end{bmatrix}.$$

Consequently the next generation matrix, $FV^{-1}$, for the sub-model (7) is calculated as

$$\begin{bmatrix} \frac{P\beta_1}{I_LPN+N} - I_C\beta_2 - \frac{I_L\beta_2}{m_1} & -\frac{I_L\beta_2}{\alpha_1} & 0 & 0 \\ I_C\beta_2 + \frac{I_L\beta_2}{m_1} & \frac{I_L\beta_2}{\alpha_1} & 0 & 0 \\ 0 & 0 & 0 & 0 \\ 0 & 0 & 0 & 0 \end{bmatrix}. \tag{8}$$

Next with the help of $(FV^{-1} - \lambda I = 0)$. The basic reproduction parameter, $\mathbf{R_0}$ is the dominant eigenvalue of the next generation matrix (7) and has the form described in (9) as

$$\begin{aligned} \mathbf{R_0} &= \frac{1}{2\alpha_1 m_1 N}\Big(m_1\alpha_1\beta_1 + N(m_1 I_C\alpha_1 + I_L(\alpha_1 + m_1))\beta_2 \\ &+ \sqrt{({\beta_1}^2{\alpha_1}^2{m_1}^2 + 2\alpha_1 m_1 N(I_C m_1\alpha_1 + I_L(-m_1 + \alpha_1))\beta_1\beta_2 + N^2(I_C m_1\alpha_1 + I_L(m_1 + \alpha_1))^2{\beta_2}^2)}\Big). \end{aligned} \tag{9}$$

Discussion in the following sections will reflect the vital role of the basic reproduction parameter $\mathbf{R_0}$ in the description of the dynamics of the disease modeled by the system in (1). In Fig. 2, we present 3 D profile of basic reproductive number.

## Main results

Here the first part of our main results has presented which consisted on further subsections.

### *Computation of strengthen number*

In thousands of research paper author's have been used the reproductive number (see [48–52]) in epidemiological modeling with a few achievements and high limitations. While this idea has been used to decide either or not the spread will be serious, a few extraordinary shortcomings have been studied. Here we remark that researchers considered the mentioned value is a unique quantity that can be computed by using various strategies. Also it has been showed that reproduction number is a function of time not a fixed value. Further, the said number cannot predict about the waveness in the transmission dynamics of the disease. Therefore some alternate quantity is needed to overcome the above shortcomings. Recently, authors [53] introduced strength number to predict wave and future dynamics of the transmission dynamics. Therefore, we derive strength number associated to $PI_LI_CITRC$.

$$\frac{\partial^2}{\partial I_L^2}\frac{\beta_1}{N}\log(PI_L + 1) = -\beta_1\left(\frac{1}{NPI_L^2} + \frac{1}{N^2I_L}\right) < 0.$$

Further, we have

$$\mathfrak{F} = \begin{bmatrix} 0 \\ -\left(\beta_1\left(\frac{1}{NPI_L^2} + \frac{1}{N^2I_L}\right)\right) \end{bmatrix},$$

and

$$\mathfrak{H}^{-1} = \begin{bmatrix} \frac{A_2A_3}{A_1A_2A_3 + A_2I_L\beta_2A_3} & 0 & 0 \\ -\frac{A_3\alpha_2}{A_1A_2A_3 + A_2I_L\beta_2A_3} & \frac{A_1A_3 + I_L\beta_2A_3}{A_1A_2A_3 + A_2I_L\beta_2A_3} & 0 \\ 0 & 0 & \frac{A_1A_2 + I_L\beta_2A_2}{A_1A_2A_3 + A_2I_L\beta_2A_3} \end{bmatrix},$$

where

$$\begin{aligned} A_1 &= -(\alpha_2 - \gamma_2 - \mu) \\ A_2 &= -(\alpha_3 - \gamma_3 + \mu) \\ A_3 &= -\delta_2^* + \mu. \end{aligned}$$

Using Mathematica program for finding $\det(\mathfrak{F}\mathfrak{H}^{-1} - \lambda I) = 0$. The resultant strength number take the form

$$\mathfrak{R}_S = -\frac{N\beta_1 + I_LP\beta_1}{A_1{I_L}^2PN^2} < 0.$$

$\mathfrak{R}_S < 0$ leads to best result that will more affirmed using different analysis comprising in finding local maxima and local minima and inflection point. Best conclusion can be get, when the obtaining strength number is less than zero, That it will further be affirmed using an alternative analysis comprising in establishing the local minima, local maxima, and inflection points. In this manner, having negative strength number means that the model $PI_LI_CITRC$ will have a solitary magnitude, either greatest or maximum point with infectious points indicating a single infection will diminish quickly from the decease free equilibrium and with renewal process the contamination will raise after a minimum point and afterward be balanced or stop later on. This will be affirmed while concentrating on indication of second derivative of infectious classes.

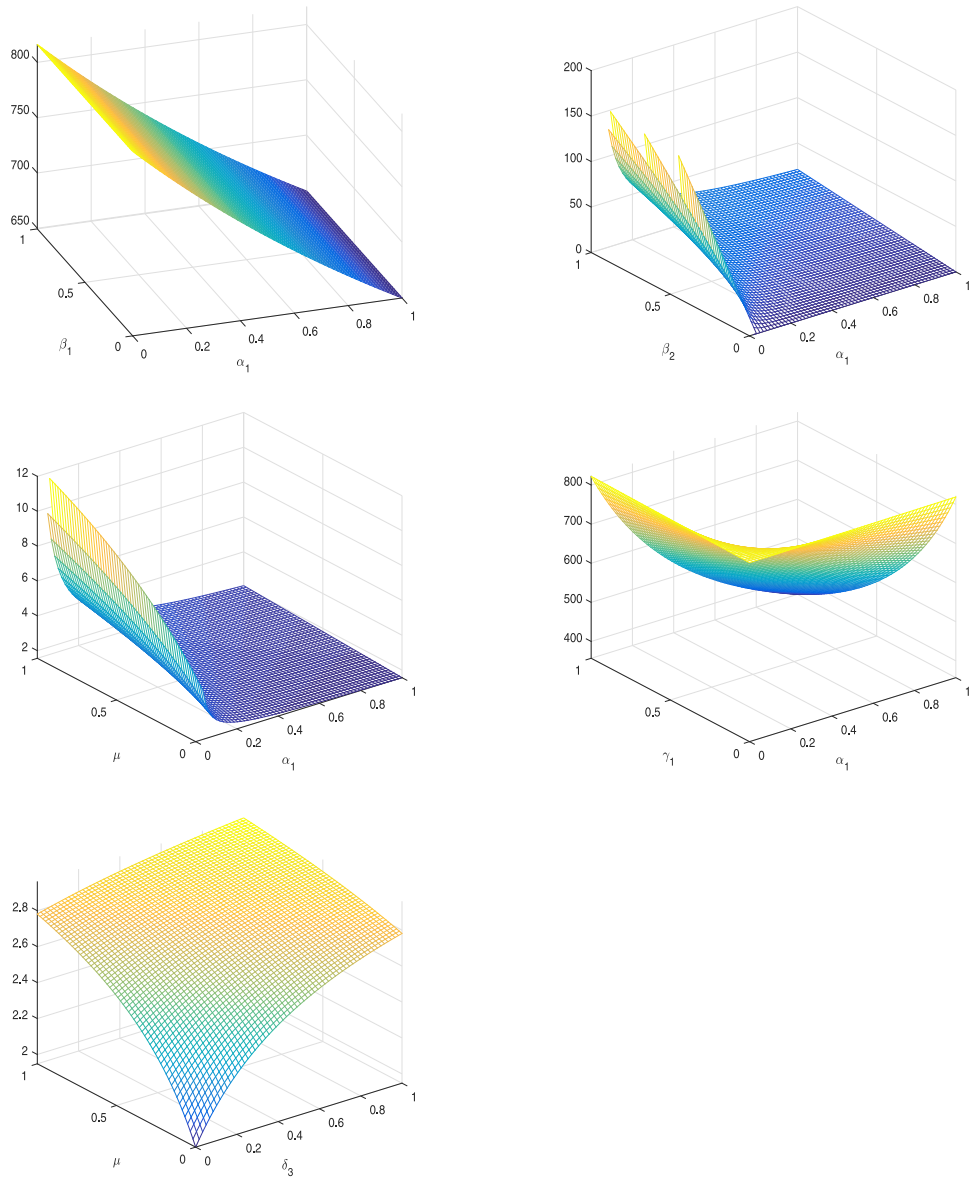


**Fig. 2.** Three dimensional plots of the basic reproduction number versus various parameters of the model (1).

*First derivative test for Lyaponove*

**Theorem 3.** *For endemic Lyaponove function [54]* $\{P, I_L, I_C, I, T, R, C\}$*, one has is* $\mathcal{L} < 0$*, when* $\mathbf{R_0} > 0$*, then* $\mathcal{E}^*$ *of proposed model is globally asymptotically stable [55].*

**Proof.** Let Lyaponove function be defined as

$$\begin{aligned}\mathcal{L}(P^*, I_L^*, I_C^*, I^*, T^*, R^*, C^*) = &\left(P - P^* - P^* \log \frac{P^*}{P}\right) + \left(I_L - I_L^* - I_L^* \log \frac{I_L^*}{I_L}\right)\\ &+ \left(I_C - I_C^* - I_C^* \log \frac{I_C^*}{I_C}\right) + \left(I - I^* - I^* \log \frac{I^*}{I}\right)\\ &+ \left(T - T^* - T^* \log \frac{T^*}{T}\right) + \left(R - R^* - R^* \log \frac{R^*}{R}\right)\\ &+ \left(C - C^* - C^* \log \frac{C^*}{C}\right).\end{aligned}$$

Differentiate both side with respect to $t$, we get

$$\begin{aligned}\frac{d\mathcal{L}}{dt} &= P'\left(\frac{P-P^*}{P}\right) + I_L'\left(\frac{I_L-I_L^*}{I_L}\right)\\ &+ I_C'\left(\frac{I_C-I_C^*}{I_C}\right) + I'\left(\frac{I-I^*}{I}\right)\\ &+ T'\left(\frac{T-T^*}{T}\right) + R'\left(\frac{R-R^*}{R}\right)\\ &+ C'\left(\frac{C-C^*}{C}\right).\end{aligned}$$

Put $P', I_L', I_C', I', T', R', C'.$, from (1), one has

$$\begin{aligned}\frac{d\mathcal{L}}{dt} &= \left(\Lambda - \frac{\beta_1}{N}\log(PI_L+1) + \delta_1 T + \delta_2^* C - \mu P\right)\left(\frac{P-P^*}{P}\right)\\ &+ \left(\frac{\beta_1}{N}\log(PI_L+1) - \beta_2 I_L I_C - (\alpha_1+\delta_3+\gamma_1+\mu)I_L\right)\left(\frac{I_L-I_L^*}{I_L}\right)\\ &+ \left(\beta_2 I_L I_C - \alpha_2 I_C - (\gamma_2+\mu)I_C + \alpha_1 I_L\right)\left(\frac{I_C-I_C^*}{I_C}\right)\\ &+ \left(\alpha_2 I_C - (\alpha_3+\gamma_3-\mu)I\right)\left(\frac{I-I^*}{I}\right)\\ &+ \left(\delta_3 I_L - \delta_4 T - (\delta_1+\mu)T + \alpha_3 I - \delta_5 T\right)\left(\frac{T-T^*}{T}\right)\\ &+ \left(\delta_4 T - \delta_2^* C - \mu C\right)\left(\frac{C-C^*}{C}\right) + \left(\delta_5 T - \mu R\right)\left(\frac{R-R^*}{R}\right).\end{aligned}$$

Replace $P = P - P^*, I_L = I_L - I_L^*, I_C = I_C - I_C^*, I = I - I^*, T = T - T^*, R = R - R^*, C = C - C^*$.

By long algebraic manipulation and rearranging the positive, negative terms we get

$$\begin{aligned}\frac{d\mathcal{L}}{dt} &= N\left(\frac{P-P^*}{P}\right) - \frac{\beta_1}{N}\log\left((P-P^*)(I_L-I_L^*)+1\right)\left(\frac{P-P^*}{P}\right) + \delta_1\left(T-T^*\right)\left(\frac{P-P^*}{P}\right)\\ &+ \delta_2^*\left(C-C^*\right)\left(\frac{P-P^*}{P}\right) - \frac{\mu}{P}\left(\frac{(P-P^*)^2}{P}\right) + \frac{\beta_1}{NI_L}\log\left((P-P^*)(I-I^*)+1\right)\left(\frac{P-P^*}{P}\right)(I_L-I_L^*)\\ &- \beta_2\left(\frac{\left(I_L-I_L^*\right)^2}{I_L}\right)\left(I_C-I_C^*\right) - \left(\frac{\left(I_L-I_L^*\right)^2}{I_L}\right)\left(\alpha_1+\delta_3+\gamma_1+\mu\right) + \beta_2\left(\frac{\left(I_C-I_C^*\right)^2}{I_C}\right)\left(I_L-I_L^*\right)\\ &- \left(\frac{\left(I_C-I_C^*\right)^2}{I_C}\right)\left(\gamma_2+\alpha_2\right) + \mu\left(\frac{\left(I_C-I_C^*\right)^2}{I_C}\right)\\ &+ \alpha_1\left(\frac{\left(I_C-I_C^*\right)}{I_C}\right)\left(I_L-I_L^*\right) + \alpha_2\left(\frac{I-I^*}{I}\right)\left(I_C-I_C^*\right)\\ &- \left(\frac{I-I^*}{I}\right)\left(\gamma_3+\alpha_3\right) + \mu\left(\frac{(I-I^*)^2}{I}\right) + \delta_3\left(\frac{T-T^*}{T}\right)\left(I_L-I_L^*\right)\\ &- \left(\frac{(T-T^*)^2}{T}\right)\left(\alpha_1+\delta_4+\delta_5\right) + \mu\left(\frac{(T-T^*)^2}{T}\right)\\ &+ \alpha_3\left(\frac{T-T^*}{T}\right)\left(I-I^*\right) + \delta_4\left(\frac{C-C^*}{C}\right)\left(T-T^*\right) - \left(\frac{(C-C^*)^2}{C}\right)\left(\mu+\delta_2^*\right)\\ &+ \delta_2\left(\frac{R-R^*}{R}\right)\left(T-T^*\right) - \mu\left(\frac{(R-R^*)}{R}\right).\end{aligned}$$

For simplicity we let $\frac{d\mathcal{L}}{dt} = \xi_1 - \xi_2$, such that

$$\begin{aligned}\xi_1 &= N\left(\frac{P-P^*}{P}\right) + \delta_1\left(T-T^*\right)\left(\frac{P-P^*}{P}\right) + \delta_2^*\left(C-C^*\right)\left(\frac{P-P^*}{P}\right)\\ &+ \frac{\beta_1}{NI_L}\log\left((P-P^*)(I-I^*)+1\right)\left(\frac{P-P^*}{P}\right)(I_L-I_L^*)\\ &+ \beta_2\left(\frac{\left(I_C-I_C^*\right)^2}{I_C}\right)\left(I_L-I_L^*\right) + \mu\left(\frac{\left(I_C-I_C^*\right)^2}{I_C}\right)\\ &+ \alpha_1\left(\frac{\left(I_C-I_C^*\right)}{I_C}\right)\left(I_L-I_L^*\right)\\ &+ \alpha_2\left(\frac{I-I^*}{I}\right)\left(I_C-I_C^*\right)\mu\left(\frac{(I-I^*)^2}{I}\right)\\ &+ \delta_3\left(\frac{T-T^*}{T}\right)\left(I_L-I_L^*\right) + \mu\left(\frac{(T-T^*)^2}{T}\right)\end{aligned}$$

$$+\ \alpha_3\left(\frac{T-T^*}{T}\right)(I-I^*)+\delta_4\left(\frac{C-C^*}{C}\right)(T-T^*)+\delta_2\left(\frac{R-R^*}{R}\right)(T-T^*)$$

$$\xi_2 = \frac{\beta_1}{N}\log\left((P-P^*)(I_L-I_L^*)+1\right)\left(\frac{P-P^*}{P}\right)+\frac{\mu}{P}\left(\frac{(P-P^*)^2}{P}\right)+\beta_2\left(\frac{\left(I_L-I_L^*\right)^2}{I_L}\right)(I_C-I_C^*)$$
$$+\left(\frac{\left(I_L-I_L^*\right)^2}{I_L}\right)(\alpha_1+\delta_3+\gamma_1+\mu)+\left(\frac{\left(I_C-I_C^*\right)^2}{I_C}\right)(\gamma_2+\alpha_2)+\left(\frac{I-I^*}{I}\right)(\gamma_3+\alpha_3)$$
$$+\left(\frac{(T-T^*)^2}{T}\right)(\alpha_1+\delta_4+\delta_5)+\left(\frac{(C-C^*)^2}{C}\right)(\mu+\delta_2^*).$$

Hence we get the result that if $\xi_1<\xi_2$ this yields $\frac{d\mathcal{L}}{dt}<0$. But $\xi_1-\xi_2=0$,
if $P=P-P^*, I_L=I_L-I_L^*, I_C=I_C-I_C^*, I=I-I^*, T=T-T^*, R=R-R^*, C=C-C^*$ which implies that $\frac{d\mathcal{L}}{dt}=0$.
We concluded the largest compact invariant set for the proposed model in

$$\{(P^*, I_L^*, I_C^*, I^*, T^*, R^*, C^*)\in\mho : \frac{d\mathcal{L}}{dt}=0\}$$

is the point $E^*$, of endemic equilibrium. Using the concept applied in [56], one has $E^*$ is globally asymptotically stable in the $\mho$, if $\xi_1<\xi_2$. □

*Second derivative of Lyapunov*

While the indication of the first derivative of a Lyapunov function assists with valuing the stability, one ought to take note of that, analysis of first derivative of a given function cannot completely assist to understand the variabilities of the function under study. Further investigation are expected to every one of the particularities of the varieties. We subsequently present an analysis of second derivative of the related Lyapunov function of our new model.

$$\frac{d\mathcal{L}}{dt} = P'\left(1-\frac{P^*}{P}\right)+I_L'\left(1-\frac{I_L^*}{I_L}\right)+I_C'\left(1-\frac{I_C^*}{I_C}\right)+I'\left(1-\frac{I^*}{I}\right)+T'\left(1-\frac{T^*}{T}\right)$$
$$+\ R'\left(1-\frac{R^*}{R}\right)+C'\left(1-\frac{C^*}{C}\right).$$

$$\frac{d^2\mathcal{L}}{dt^2} = \left(\frac{P'}{P}\right)^2P^*+\left(\frac{I_L'}{I_L}\right)^2I_L^*+\left(\frac{I_C'}{I_C}\right)^2I_C^*+\left(\frac{I'}{I}\right)^2I^*+\left(\frac{T'}{T}\right)^2T^*+\left(\frac{R'}{R}\right)^2R^*+\left(\frac{C'}{C}\right)^2C^*$$
$$+\ P''\left(1-\frac{P^*}{P}\right)+I_L''\left(1-\frac{I_L^*}{I_L}\right)+I_C''\left(1-\frac{I_C^*}{I_C}\right)+I''\left(1-\frac{I^*}{I}\right)+T''\left(1-\frac{T^*}{T}\right)$$
$$+\ R''\left(1-\frac{R^*}{R}\right)+C''\left(1-\frac{C^*}{C}\right).$$

Put $P'', I_L'', I_C'', I'', T'', R'', C''$ in the above equation, where

$$P'' = -\beta_1\left(\frac{(PI_L'+I_LP')}{N(PI_L+1)}\right)-\beta_1N'log\left(PI_L+1\right)-\mu P'+\delta_1T'+\delta_2^*C'$$
$$I_L'' = \beta_1\left(\frac{(PI_L'+I_LP')}{N(PI_L+1)}\right)+\beta_1N'log\left(PI_L+1\right)-\beta_2\left(I_LI_C'+I_CI_L'\right)-I_L'(\alpha_1+\delta_3+\mu+\gamma_1)$$
$$I_C'' = \beta_2\left(I_LI_C'+I_CI_L'\right)-\alpha_2I_C'-I_C'\left(\gamma_2+\mu\right)+\alpha_1I_L'$$
$$I'' = \alpha_2I_C'-I'\left(\alpha_3+\gamma_3-\mu\right)$$
$$T'' = \delta_3I_L'-\delta_4T'-\left(\delta_1-\mu\right)T'+\alpha_3I'-\delta_5T'$$
$$R'' = \delta_5T'-\mu R'$$
$$C'' = \delta_4T'+\delta_2^*C'-\mu C'.$$

We have

$$\begin{cases}\frac{d^2\mathcal{L}}{dt^2}=\left(\frac{P'}{P}\right)^2P^*+\left(\frac{I_L'}{I_L}\right)^2I_L^*+\left(\frac{I_C'}{I_C}\right)^2I_C^*+\left(\frac{I'}{I}\right)^2I^*+\left(\frac{T'}{T}\right)^2T^*+\left(\frac{R'}{R}\right)^2R^*+\left(\frac{C'}{C}\right)^2C^*\\ +\left(1-\frac{P^*}{P}\right)\left(-\beta_1\left(\frac{(PI_L'+I_LP')}{N(PI_L+1)}\right)-\beta_1N'\log\left(PI_L+1\right)-\mu P'+\delta_1T'+\delta_2^*C'\right)\\ +\left(1-\frac{I_L^*}{I_L}\right)\left(\beta_1\left(\frac{(PI_L'+I_LP')}{N(PI_L+1)}\right)+\beta_1N'log\left(PI_L+1\right)-\beta_2\left(I_LI_C'+I_CI_L'\right)-I_L'(\alpha_1+\delta_3+\mu+\gamma_1)\right)\\ +\left(1-\frac{I_C^*}{I_C}\right)\left(\beta_2\left(I_LI_C'+I_CI_L'\right)-\alpha_2I_C'-I_C'\left(\gamma_2+\mu\right)+\alpha_1I_L'\right)+\left(1-\frac{I^*}{I}\right)\left(\alpha_2I_C'-I'\left(\alpha_3+\gamma_3-\mu\right)\right)\\ +\left(1-\frac{T^*}{T}\right)\left(\delta_3I_L'-\delta_4T'-\left(\delta_1-\mu\right)T'+\alpha_3I'-\delta_5T'\right)+\left(1-\frac{R^*}{R}\right)\left(\delta_5T'-\mu R'\right)\\ +\left(1-\frac{C^*}{C}\right)\left(\delta_4T'+\delta_2^*C'-\mu C'\right).\end{cases}$$

Similarly using the values $\{P', I_L', I_C', I', T', R', C'\}$, one has

$$
\begin{aligned}
\frac{d^2\mathcal{L}}{dt^2} &= \left(\frac{\left(N-\frac{\beta_1}{N}\log(PI_L+1)+\delta_2 T+\delta_2^* C-\mu P\right)}{P}\right)^2 P^* \\
&+\left(\frac{\left(\frac{\beta_1}{N}\log(PI_L+1)-\beta_2 I_L I_C-(\alpha_1+\delta_3+\gamma_1+\mu)I_L\right)}{I_L}\right)^2 I_L^* \\
&+\left(\frac{\left(\beta_2 I_L I_C-\alpha_2 I_C-(\gamma_2+\mu)I_C+\alpha_1 I_L\right)}{I_C}\right)^2 I_C^* \\
&+\left(\frac{\left(\alpha_2 I_C-(\alpha_3\gamma_3-\mu)I\right)}{I}\right)^2 I^* + \left(\frac{\left(\delta_3 I_L-\delta_4 T-(\delta_1-\mu)T+\alpha_3 I-\delta_5 T\right)}{T}\right)^2 T^* \\
&+\left(\frac{\left(\delta_5 T-\mu R\right)}{R}\right)^2 R^* + \left(\frac{\left(\delta_4 T-\delta_2^* C-\mu C\right)}{C}\right)^2 C^* \\
&-\left(1-\frac{P^*}{P}\right)\beta_1\left(\frac{P\left(\frac{\beta_1}{N}\log(PI_L+1)-\beta_2 I_L I_C-(\alpha_1+\delta_3+\gamma_1+\mu)I_L\right)}{N(PI_L+1)}\right. \\
&\left.+\frac{I_L\left(N-\frac{\beta_1}{N}\log(PI_L+1)+\delta_2 T+\delta_2^* C-\mu P\right)}{N(PI_L+1)}\right) \\
&-\left(1-\frac{P^*}{P}\right)\beta_1\left(N-\mu N-\gamma_1 I_L+\alpha_1 I_C-\gamma_2 I_C-\gamma_3 I\right)\log\left(PI_L+1\right) \\
&-\left(1-\frac{P^*}{P}\right)\mu\left(N-\frac{\beta_1}{N}\log(PI_L+1)+\delta_2 T+\delta_2^* C-\mu P\right) \\
&+\left(1-\frac{P^*}{P}\right)\delta_1\left(\delta_3 I_L-\delta_4 T-(\delta_1-\mu)\right)T \\
&+\left(1-\frac{P^*}{P}\right)\delta_1\left(\alpha_3 I-\delta_5 T\right)+\left(1-\frac{P^*}{P}\right)\delta_2^*\left(\delta_4 T-\delta_2^* C-\mu C\right) \\
&+\left(1-\frac{I_L^*}{I_L}\right)\beta_1\left(\frac{P\left(\frac{\beta_1}{N}\log(PI_L+1)-\beta_2 I_L I_C-(\alpha_1+\delta_3+\gamma_1+\mu)I_L\right)}{N(PI_L+1)}\right. \\
&\left.+\frac{I_L\left(N-\frac{\beta_1}{N}\log(PI_L+1)+\delta_2 T+\delta_2^* C-\mu P\right)}{N(PI_L+1)}\right) \\
&+\left(1-\frac{I_L^*}{I_L}\right)\beta_1\left(N-\mu N-\gamma_1 I_L+\alpha_1 I_C-\gamma_2 I_C-\gamma_3 I\right) log\left(PI_L+1\right) \\
&-\left(1-\frac{I_L^*}{I_L}\right)\beta_2 I_L\left(\beta_2 I_L I_C-\alpha_2 I_C-(\gamma_2+\mu)I_C+\alpha_1 I_L\right) \\
&+\left(1-\frac{I_L^*}{I_L}\right)\beta_2 I_C\left(\frac{\beta_1}{N}\log(PI_L+1)-\beta_2 I_L I_C-(\alpha_1+\delta_3+\gamma_1+\mu)I_L\right) \\
&-\left(1-\frac{I_L^*}{I_L}\right)\left(\frac{\beta_1}{N}\log(PI_L+1)-\beta_2 I_L I_C-(\alpha_1+\delta_3+\gamma_1+\mu)I_L\right)(\alpha_1+\delta_3+\mu+\gamma_1) \\
&+\left(1-\frac{I_C^*}{I_C}\right)\beta_2 I_L\left(\beta_2 I_L I_C-\alpha_2 I_C-(\gamma_2+\mu)I_C+\alpha_1 I_L\right) \\
&+\left(1-\frac{I_C^*}{I_C}\right)\beta_2 I_C\left(\frac{\beta_1}{N}\log(PI_L+1)-\beta_2 I_L I_C-(\alpha_1+\delta_3+\gamma_1+\mu)I_L\right) \\
&-\alpha_2\left(\beta_2 I_L I_C-\alpha_2 I_C-(\gamma_2+\mu)I_C+\alpha_1 I_L\right) \\
&-\left(\beta_2 I_L I_C-\alpha_2 I_C-(\gamma_2+\mu)I_C+\alpha_1 I_L\right)\left(\gamma_2+\mu\right) \\
&+\alpha_1\left(\frac{\beta_1}{N}\log(PI_L+1)-\beta_2 I_L I_C-(\alpha_1+\delta_3+\gamma_1+\mu)I_L\right) \\
&+\left(1-\frac{I^*}{I}\right)\alpha_2\left(\beta_2 I_L I_C-\alpha_2 I_C-(\gamma_2+\mu)I_C+\alpha_1 I_L\right) \\
&-\left(1-\frac{I^*}{I}\right)\left(\alpha_2 I_C-(\alpha_3+\gamma_3-\mu)I\right)\left(\alpha_3+\gamma_3-\mu\right) \\
&+\left(1-\frac{T^*}{T}\right)\delta_3\left(\frac{\beta_1}{N}\log(PI_L+1)-\beta_2 I_L I_C-(\alpha_1+\delta_3+\gamma_1+\mu)I_L\right) \\
&-\left(1-\frac{T^*}{T}\right)\delta_4\left(\delta_3 I_L-\delta_4 T-(\delta_1-\mu)T+\alpha_3 I-\delta_5 T\right)
\end{aligned}
$$

$$
\begin{aligned}
&- \left(1-\frac{T^*}{T}\right)(\delta_1-\mu)\left(\delta_3 I_L-\delta_4 T-(\delta_1-\mu)T+\alpha_3 I-\delta_5 T\right)\\
&+ \left(1-\frac{T^*}{T}\right)\alpha_3\left(\alpha_2 I_C-(\alpha_3+\gamma_3-\mu)I\right)-\left(1-\frac{T^*}{T}\right)\delta_5\left(\delta_3 I_L-\delta_4 T-(\delta_1-\mu)T+\alpha_3 I-\delta_5 T\right)\\
&+ \left(1-\frac{R^*}{R}\right)\left(\delta_5\left(\delta_3 I_L-\delta_4 T-(\delta_1-\mu)T+\alpha_3 I-\delta_5 T\right)-\mu\left(\delta_5 T-\mu R\right)\right)\\
&+ \left(1-\frac{C^*}{C}\right)\Bigg(\delta_4\left(\delta_3 I_L-\delta_4 T-(\delta_1-\mu)T+\alpha_3 I-\delta_5 T\right)\\
&+ (\delta_2^*-\mu)\left(\delta_4 T-\delta_2^* C-\mu C\right)\Bigg).
\end{aligned}
$$

For our simplification and rearranging, we may write

$$\frac{d^2\mathcal{L}}{dt^2}=\mathfrak{U}_1-\mathfrak{U}_2,$$

where

$$
\begin{aligned}
\mathfrak{U}_1 =\ & \Delta'(P,I_L,I_C,I,T,R,C)+\frac{\beta_1\beta_2 I_C}{N}\left(1-\frac{P^*}{P}\right)\log(PI_L+1)\\
&+\frac{\beta_1}{N}\left(1-\frac{P^*}{P}\right)(\alpha_1+\delta_3+\mu+\gamma_1)\\
&+\frac{{\beta_1}^2}{N^2P}\left(1-\frac{P^*}{P}\right)\log(PI_L+1)+\frac{\beta_1\mu}{N}\left(1-\frac{P^*}{P}\right)+\beta_1 N\mu\left(1-\frac{P^*}{P}\right)\log(PI_L+1)\\
&+\beta_1\gamma_1 I_L\left(1-\frac{P^*}{P}\right)\log(PI_L+1)+\beta_1\gamma_2 I_C\left(1-\frac{P^*}{P}\right)\log(PI_L+1)\\
&+\beta_1\gamma_3 I\left(1-\frac{P^*}{P}\right)\log(PI_L+1)+\frac{\beta_1\mu}{N}\left(1-\frac{P^*}{P}\right)\log(PI_L+1)+P\mu^2\left(1-\frac{P^*}{P}\right)\\
&+\frac{{\beta_1}^2}{N^2 I_L}\left(1-\frac{{I_L}^*}{I_L}\right)\log(PI_L+1)+\frac{\beta_1}{P}\left(1-\frac{{I_L}^*}{I_L}\right)+\frac{\beta_1\delta_1 T}{NP}\left(1-\frac{{I_L}^*}{I_L}\right)+\delta_1\delta_3 I_L\left(1-\frac{P^*}{P}\right)\\
&+\delta_1\alpha_3 I\left(1-\frac{P^*}{P}\right)+\delta_2^*\delta_4\left(1-\frac{P^*}{P}\right)+N\beta_1\left(1-\frac{{I_L}^*}{I_L}\right)\log(PI_L+1)\\
&+\beta_1\alpha_1 I_C\left(1-\frac{{I_L}^*}{I_L}\right)\log(PI_L+1)+\beta_2\alpha_2 I_C I_L\left(1-\frac{{I_L}^*}{I_L}\right)+\beta_2 I_C I_L\left(1-\frac{{I_L}^*}{I_L}\right)(\gamma_2+\mu)\\
&+\frac{\beta_1 I_C}{N}\log(PI_L+1)+(\alpha_2 I_C)(\alpha_1+\delta_3+\mu+\gamma_1)\left(1-\frac{{I_L}^*}{I_L}\right)\\
&+I_C(\alpha_1+\delta_3+\mu+\gamma_1)\left(1-\frac{{I_L}^*}{I_L}\right)+\alpha_2\beta_2 I_C I_L\left(1-\frac{I^*}{I}\right)+\alpha_1\alpha_2 I_L\left(1-\frac{I^*}{I}\right)\\
&+(\alpha_3-\mu+\gamma_3)^2 I\left(1-\frac{I^*}{I}\right)+\frac{\delta_1\beta_1}{N}\left(1-\frac{T^*}{T}\right)\log(PI_L+1)\\
&+{\delta_4}^2 T\left(1-\frac{T^*}{T}\right)+\delta_4 T(\delta_1-\mu)\left(1-\frac{T^*}{T}\right)+\delta_4\delta_5 T\left(1-\frac{T^*}{T}\right)\\
&+T(\delta_1-\mu)^2\left(1-\frac{T^*}{T}\right)+T\delta_5(\delta_1-\mu)\left(1-\frac{T^*}{T}\right)+\delta_3\delta_5 I_L\left(1-\frac{R^*}{R}\right)\\
&+\alpha_3\delta_5 I\left(1-\frac{R^*}{R}\right)+\mu^2 R\left(1-\frac{R^*}{R}\right)+\delta_2^*\delta_4 T\left(1-\frac{C^*}{C}\right)\\
&+\delta_2^*\mu C\left(1-\frac{C^*}{C}\right)+\mu^2 C\left(1-\frac{C^*}{C}\right),
\end{aligned}
$$

and

$$
\begin{aligned}
\mathfrak{U}_2 =\ & \frac{{\beta_1}^2}{N^2 I_L}\left(1-\frac{P^*}{P}\right)\log(PI_L+1)+\frac{\beta_1}{P}\left(1-\frac{P^*}{P}\right)+\frac{\beta_1\delta_1 T}{NP}\left(1-\frac{P^*}{P}\right)\\
&+\frac{\beta_1\delta_2^* C}{NP}\left(1-\frac{P^*}{P}\right)+\beta_1 N I_L\left(1-\frac{P^*}{P}\right)\log(PI_L+1)\\
&+\beta_1\alpha_1 I_C\left(1-\frac{P^*}{P}\right)\log(PI_L+1)+\mu\delta_1 T\left(1-\frac{P^*}{P}\right)\\
&+\mu\delta_2^* C\left(1-\frac{P^*}{P}\right)+\frac{\beta_1\beta_2 I_C}{N}\left(1-\frac{{I_L}^*}{I_L}\right)\log(PI_L+1)\\
&+\frac{\beta_1}{N}(\alpha_1+\delta_3+\mu+\gamma_1)\left(1-\frac{{I_L}^*}{I_L}\right)+\frac{\mu\beta_1}{N}\left(1-\frac{{I_L}^*}{I_L}\right)\\
&+\delta_1\delta_4 T\left(1-\frac{P^*}{P}\right)+\delta_1 T(\delta_1-\mu)\left(1-\frac{P^*}{P}\right)+\delta_1\delta_5 T\left(1-\frac{P^*}{P}\right)\\
&+\delta_2^*\mu C\left(1-\frac{P^*}{P}\right)+\beta_1\mu N\log(PI_L+1)\left(1-\frac{{I_L}^*}{I_L}\right)+\beta_1 I_L\gamma_1\log(PI_L+1)\left(1-\frac{{I_L}^*}{I_L}\right)
\end{aligned}
$$

**Table 2**
Nomenclatures of (1) and numerical values.

| Nomenclature | Numerical values |
|---|---|
| $P(0)$ | 40 |
| $I_L(0)$ | 20 |
| $I_C(0)$ | 15 |
| $I(0)$ | 10 |
| $T(0)$ | 10 |
| $C(0)$ | 5 |
| $R(0)$ | 0 |
| $\Lambda$ | 0.0020 |
| $\beta_1$ | 0.00012 |
| $\beta_2$ | 0.0020 |
| $\delta_1$ | 0.0032 |
| $\delta_2^*$ | 0.00233 |
| $\delta_3$ | 0.00462 |
| $\delta_4$ | 0.00023 |
| $\delta_5$ | 0.000123 |
| $\mu$ | 0.05 |
| $\alpha_1$ | =0.0010 |
| $\alpha_2$ | =0.0045 |
| $\alpha_3$ | 0.000123 |
| $\gamma_1$ | 0.007 |
| $\gamma_2$ | 0.00023 |
| $\gamma_3$ | 0.00034 |

$$
\begin{aligned}
&+ \delta_2^* C\left(1-\frac{P^*}{P}\right) + \beta_1 I_L \gamma_2 \log(PI_L+1)\left(1-\frac{{I_L}^*}{I_L}\right) + \beta_1 I \gamma_3 \log(PI_L+1)\left(1-\frac{{I_L}^*}{I_L}\right)\\
&+ I_C {I_L}^2 {\beta_2}^2\left(1-\frac{{I_L}^*}{I_L}\right) + \alpha_1 {I_L}^2 \beta_2\left(1-\frac{{I_L}^*}{I_L}\right) + \beta_2 I_L {I_C}^2 + (\alpha_1+\delta_3+\mu+\gamma_1) I_L I_C\\
&+ (\alpha_1+\delta_3+\mu+\gamma_1)\beta_2 I_L I_C\left(1-\frac{{I_L}^*}{I_L}\right) + (\alpha_1+\delta_3+\mu+\gamma_1)\alpha_1 I_L\left(1-\frac{{I_L}^*}{I_L}\right)\\
&+ {\alpha_2}^2 I_C\left(1-\frac{{I_L}^*}{I_L}\right) + \alpha_2 I_C(\gamma_2+\mu)\left(1-\frac{{I_L}^*}{I_L}\right) + \delta_3 I_C(\alpha_3-\mu+\gamma_3)\left(1-\frac{I^*}{I}\right)\\
&+ \beta_2 I_L I_C \delta_3\left(1-\frac{T^*}{T}\right) + \delta_3 I_L(\alpha_1+\delta_3+\mu+\gamma_1)\left(1-\frac{T^*}{T}\right) + \delta_3\delta_4 I_L\left(1-\frac{T^*}{T}\right)\\
&+ \delta_4\alpha_3 I\left(1-\frac{T^*}{T}\right) + \delta_3 I_L(\delta_1-\mu)\left(1-\frac{T^*}{T}\right) + \alpha_3 I(\delta_1-\mu)\left(1-\frac{T^*}{T}\right)\\
&+ \delta_3\delta_5 I\left(1-\frac{T^*}{T}\right) + \delta_4\delta_5 T\left(1-\frac{R^*}{R}\right) + T\delta_5(\delta_1-\mu)\left(1-\frac{R^*}{R}\right) + {\delta_5}^2 T\left(1-\frac{T^*}{T}\right)\\
&+ {\delta_5}^2 T\left(1-\frac{R^*}{R}\right) + \delta_5 T\mu\left(1-\frac{R^*}{R}\right) + \delta_2^{*2} C\left(1-\frac{C^*}{C}\right)\\
&+ \delta_2^*\mu C\left(1-\frac{C^*}{C}\right) + \delta_4\mu T\left(1-\frac{C^*}{C}\right).
\end{aligned}
$$

It is clearly be seen that

$$If \quad \mathfrak{U}_1 > \mathfrak{U}_2 \quad then \frac{d^2\mathcal{L}}{dt^2} > 0, \tag{10}$$

$$If \quad \mathfrak{U}_1 < \mathfrak{U}_2 \quad then \frac{d^2\mathcal{L}}{dt^2} < 0, \tag{11}$$

$$If \quad \mathfrak{U}_1 = \mathfrak{U}_2 \quad then \frac{d^2\mathcal{L}}{dt^2} = 0. \tag{12}$$

## Numerical presentations and discussion

Now using the following values for the nomenclatures of the proposed model to simulate the results In order to simulate the outcomes using our suggested numerical scheme, we take the total population to be $N = 100$ millions and use the numerical data from Table 2. Figs. 3 and 4 show the equivalent results for the various compartments graphically, respectively. One may observe the behaviors of various compartments in the Figs. 3, and 4 above displayed of our proposed model using classical order derivative. In the previously stated circumstances, the model (1) will probably be unable to show more waves. The spread will eventually disappear without any renewal force, according to the model. However, this model has been utilized in literature to illustrate how infectious diseases propagate in several waves.

## Fractional order model and numerical simulations

Here, we attempt to investigate the proposed model under the concept of Caputo fractional order derivative for more explanation about the transmission dynamics. We set our model (1) as

$$^{C}D_t^{o} P(t) = \Lambda - \frac{\beta_1}{N}\log(PI_L+1) + \delta_1 T + \delta_2^* C - \mu P$$

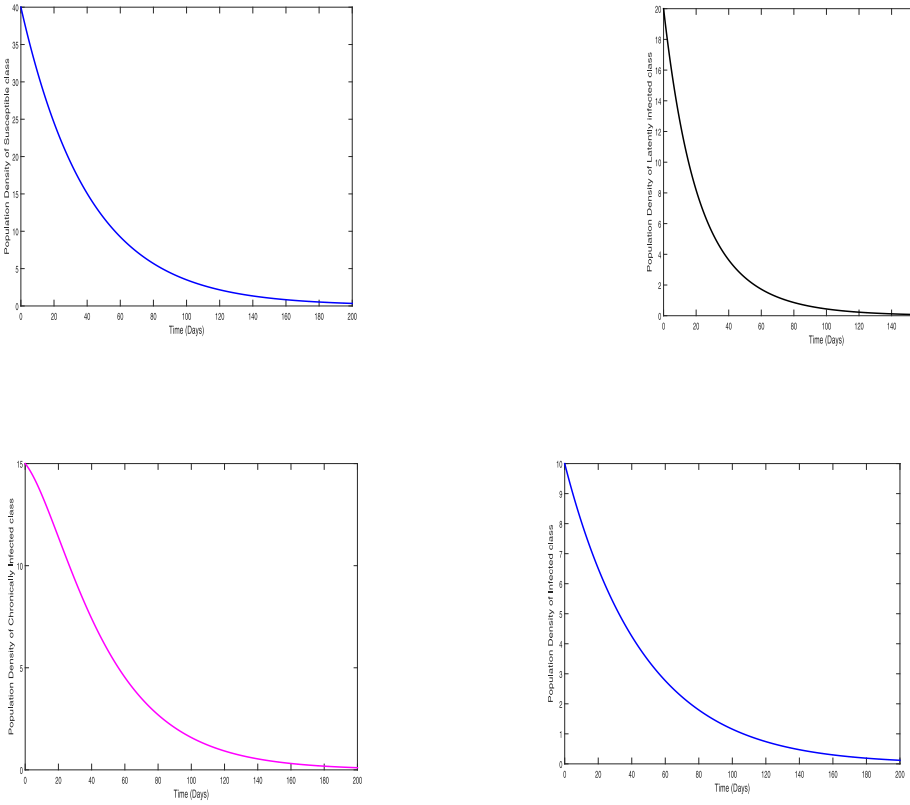


**Fig. 3.** Graphical presentation of susceptible, latently infected, chronically and infected compartments.

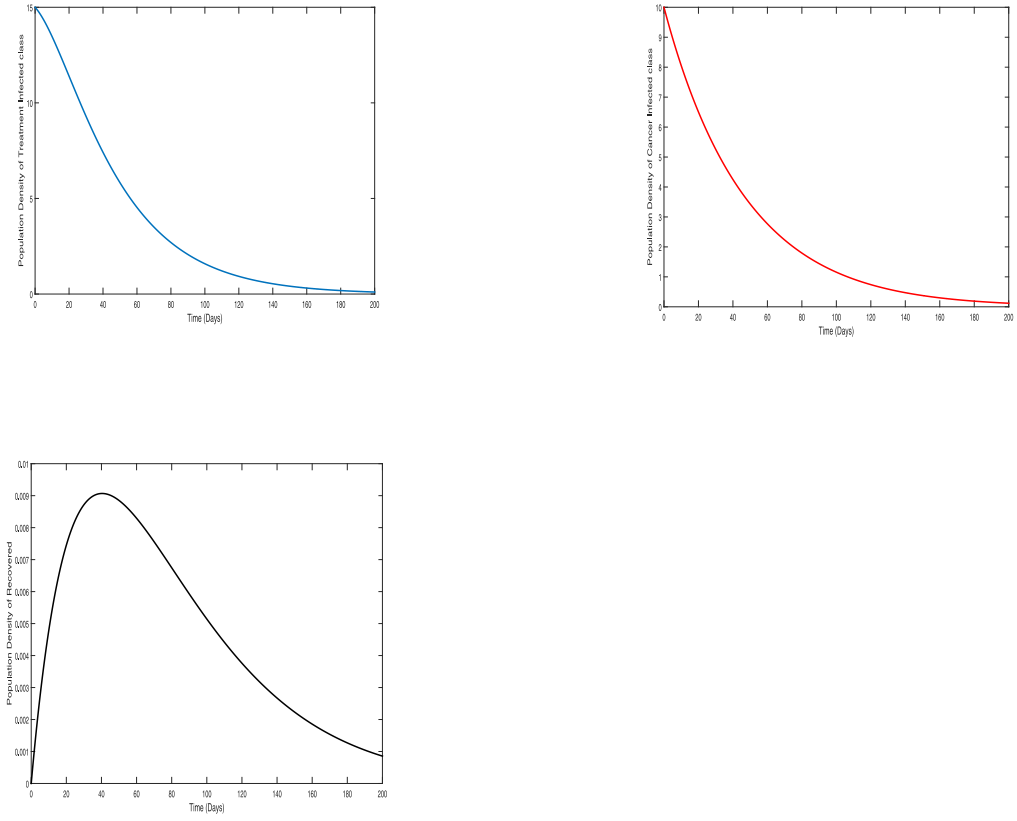


**Fig. 4.** Graphical presentation of treatment, cancer infected and recovered compartments.

$$
\begin{aligned}
{}^{C}D_t^{\varrho} I_L(t) &= \frac{\beta_1}{N}\log(PI_L+1) - \beta_2 I_L I_C - (\alpha_1+\delta_3+\gamma_1+\mu)I_L,\\
{}^{C}D_t^{\varrho} I_C(t) &= \beta_2 I_L I_C - \alpha_2 I_C - (\gamma_2+\mu)I_C + \alpha_1 I_L,\\
{}^{C}D_t^{\varrho} I(t) &= \alpha_2 I_C - (\alpha_3+\gamma_3-\mu)I,\\
{}^{C}D_t^{\varrho} T(t) &= \delta_3 I_L - \delta_4 T - (\delta_1+\mu)T + \alpha_3 I - \delta_5 T,\\
{}^{C}D_t^{\varrho} C(t) &= \delta_4 T - \delta_2^{*} C - \mu C,\\
{}^{C}D_t^{\varrho} R(t) &= \delta_5 T - \mu R,\\
P(0)>0, I_L(0) &\geq 0, I_C \geq 0, I(0)\geq 0, T(0)\geq 0, C(0)\geq 0, R(0)\geq 0.
\end{aligned} \tag{13}
$$

To simulate the model given in (13), we consider the solution (3) given in Theorem 2 by using $h$ is a step size, $t_{j+1}=(j+1)h$, and $t_j = jh$, $j = 0,1,2,\ldots.$ as

$$
P(t_{j+1}) = P_0 + \int_0^{t_{j+1}} \frac{(t_{j+1}-\varsigma)^{\varrho-1}}{\Gamma(\varrho)}\Psi(\varsigma, P(\varsigma))d\varsigma. \tag{14}
$$

To solve integral (14), authors [37] have applied two-step Lagrange interpolation and obtained the following numerical result

$$
\begin{aligned}
P_{j+1} &= P_0 + \frac{h^{\varrho}}{\Gamma(\varrho+2)}\sum_{l=0}^{j}\Psi(t_l,P_l)\begin{bmatrix}(j-l+1)^{\varrho}(j-l+2+\varrho)\\ -(j-l)^{\varrho}(j-l+2+2\varrho)\end{bmatrix}\\
&- \frac{h^{\varrho}}{\Gamma(\varrho+2)}\sum_{l=0}^{j}\Psi(t_{l-},P_{l-1})\begin{bmatrix}(j-l+1)^{\varrho+1}\\ -(j-l)^{\varrho}(j-l+1+\varrho)\end{bmatrix}.
\end{aligned} \tag{15}
$$

Repeating the same process as in (15), we establish for other compartments as follow

$$
\begin{aligned}
I_{L,j+1} &= I_{L,0} + \frac{h^{\varrho}}{\Gamma(\varrho+2)}\sum_{l=0}^{j}\Psi(t_l,I_{L,l})\begin{bmatrix}(j-l+1)^{\varrho}(j-l+2+\varrho)\\ -(j-l)^{\varrho}(j-l+2+2\varrho)\end{bmatrix}\\
&- \frac{h^{\varrho}}{\Gamma(\varrho+2)}\sum_{l=0}^{j}\Psi(t_{l-},I_{L,l-1})\begin{bmatrix}(j-l+1)^{\varrho+1}\\ -(j-l)^{\varrho}(j-l+1+\varrho)\end{bmatrix}.
\end{aligned} \tag{16}
$$

$$
\begin{aligned}
I_{C,j+1} &= I_{C,0} + \frac{h^{\varrho}}{\Gamma(\varrho+2)}\sum_{l=0}^{j}\Psi(t_l,I_{C,l})\begin{bmatrix}(j-l+1)^{\varrho}(j-l+2+\varrho)\\ -(j-l)^{\varrho}(j-l+2+2\varrho)\end{bmatrix}\\
&- \frac{h^{\varrho}}{\Gamma(\varrho+2)}\sum_{l=0}^{j}\Psi(t_{l-},I_{C,l-1})\begin{bmatrix}(j-l+1)^{\varrho+1}\\ -(j-l)^{\varrho}(j-l+1+\varrho)\end{bmatrix}.
\end{aligned} \tag{17}
$$

$$
\begin{aligned}
I_{j+1} &= I_0 + \frac{h^{\varrho}}{\Gamma(\varrho+2)}\sum_{l=0}^{j}\Psi(t_l,I_l)\begin{bmatrix}(j-l+1)^{\varrho}(j-l+2+\varrho)\\ -(j-l)^{\varrho}(j-l+2+2\varrho)\end{bmatrix}\\
&- \frac{h^{\varrho}}{\Gamma(\varrho+2)}\sum_{l=0}^{j}\Psi(t_{l-},I_{l-1})\begin{bmatrix}(j-l+1)^{\varrho+1}\\ -(j-l)^{\varrho}(j-l+1+\varrho)\end{bmatrix}.
\end{aligned} \tag{18}
$$

$$
\begin{aligned}
T_{j+1} &= T_0 + \frac{h^{\varrho}}{\Gamma(\varrho+2)}\sum_{l=0}^{j}\Psi(t_l,T_l)\begin{bmatrix}(j-l+1)^{\varrho}(j-l+2+\varrho)\\ -(j-l)^{\varrho}(j-l+2+2\varrho)\end{bmatrix}\\
&- \frac{h^{\varrho}}{\Gamma(\varrho+2)}\sum_{l=0}^{j}\Psi(t_{l-},T_{l-1})\begin{bmatrix}(j-l+1)^{\varrho+1}\\ -(j-l)^{\varrho}(j-l+1+\varrho)\end{bmatrix}.
\end{aligned} \tag{19}
$$

$$
\begin{aligned}
C_{j+1} &= C_0 + \frac{h^{\varrho}}{\Gamma(\varrho+2)}\sum_{l=0}^{j}\Psi(t_l,C_l)\begin{bmatrix}(j-l+1)^{\varrho}(j-l+2+\varrho)\\ -(j-l)^{\varrho}(j-l+2+2\varrho)\end{bmatrix}\\
&- \frac{h^{\varrho}}{\Gamma(\varrho+2)}\sum_{l=0}^{j}\Psi(t_{l-},C_{l-1})\begin{bmatrix}(j-l+1)^{\varrho+1}\\ -(j-l)^{\varrho}(j-l+1+\varrho)\end{bmatrix}.
\end{aligned} \tag{20}
$$

$$
\begin{aligned}
R_{j+1} &= R_0 + \frac{h^{\varrho}}{\Gamma(\varrho+2)}\sum_{l=0}^{j}\Psi(t_l,R_l)\begin{bmatrix}(j-l+1)^{\varrho}(j-l+2+\varrho)\\ -(j-l)^{\varrho}(j-l+2+2\varrho)\end{bmatrix}\\
&- \frac{h^{\varrho}}{\Gamma(\varrho+2)}\sum_{l=0}^{j}\Psi(t_{l-},R_{l-1})\begin{bmatrix}(j-l+1)^{\varrho+1}\\ -(j-l)^{\varrho}(j-l+1+\varrho)\end{bmatrix}.
\end{aligned} \tag{21}
$$

Using the considered numerical scheme, we present the solutions graphically for various compartments corresponding to different fractional orders in Figs. 5, 6 respectively. Here, we demonstrate that fractional order derivative has been considered in Caputo sense. The presented numerical simulations for different fractional orders tell us about the global dynamics. As the order is smaller the decay process in various compartments is faster as compared to higher fractional order. In the same way, the growth phenomenon is more faster for greater fractional order as compared to lower fractional order. Hence we concluded that smaller fractional order models are more significant for the description of those evolution process exhibiting decay in their nature. While growth process are more brilliantly be described by using larger fractional order models.

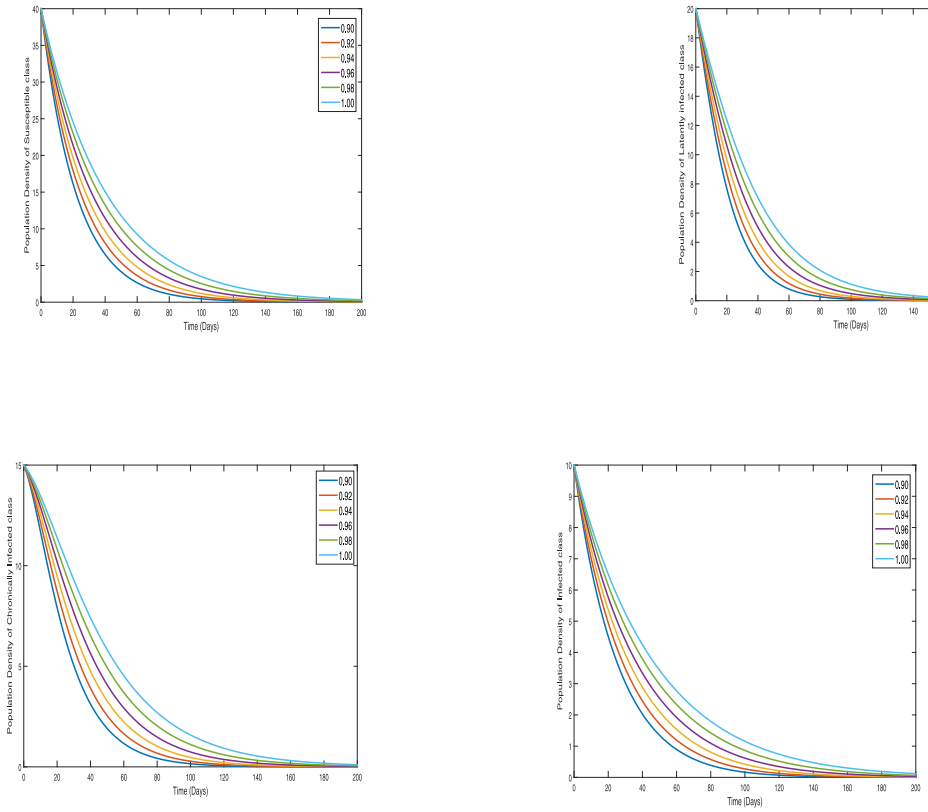


**Fig. 5.** Graphical presentation of susceptible, latently infected, chronically and infected compartments corresponding to different fractional orders.

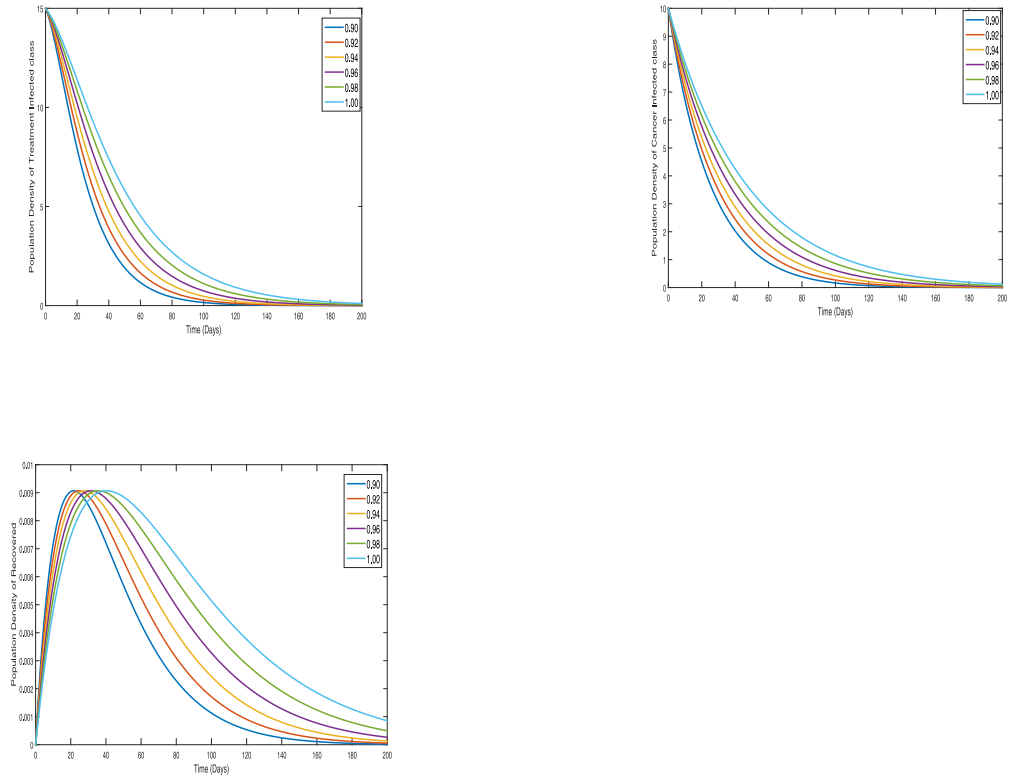


**Fig. 6.** Graphical presentation of treatment, cancer infected and recovered compartments corresponding to different fractional orders.

## Conclusion

This manuscript has been devoted to establish a detailed analysis of tobacco-cancer mathematical model using both traditional as well as fractional order concepts. The complicated dynamics of an epidemic model that addresses the spread of infectious diseases under the influence of various irresistible periods (latently, chronically, class with treatment, and infected) have been dealt with in this research effort by developing an updated mathematical model. We have proved the existence, boundedness, and positivity of the model. We have specifically looked at the main characteristics of the suggested model, which support the notion that it has properly stated. We obtained the fundamental reproduction number and investigated its impact on the various model parameters by using the well-known method called the next generation matrix procedure. We have arrived at the strength number by taking the Lyaponove function and its second derivative to detect the future prediction about the infection transmission. In addition, it has been proved that the model is locally and globally asymptotically stable according to quantitative analysis that was conducted using several techniques (first and second derivative tests, LaSalle's invariant theorem). Additionally, we have used the traditional RK-4 method to graphically present our numerical findings and established that maintaining a value for (9) smaller than one is one of the key factors in halting the spread of an infectious virus. Additionally, we have used the Euler numerical scheme to simulate the outcomes for various compartments under fractional orders derivative with Caputo power law kernel. We noted that, in contrast to the classical order depicted in Figs. 3 and 4, the dynamical behaviors of the various compartments corresponding to fractional orders are more complex and global as shown in 5 and 6, respectively. Moreover, the analysis we established here will be utilized in future to study more complex dynamical systems of various infectious disease like COVID-19, hepatitis C and B, etc.

## CRediT authorship contribution statement

**Ismail Shah:** Writing – original draft, Design, Methodology. **Eiman:** Theoretical results. **Hussam Alrabaiah:** Revised the paper, Including more literatures and updation. **Burhanettin Ozdemir:** Simulation. **Ateeq ur Rehman Irshad:** Revised, Edited.

## Declaration of competing interest

There does not exists conflict of interest.

## Data availability

No data was used for the research described in the article.

## Acknowledgments

The authors Burhanettin Ozdemir and Ateeq ur Rehman Irshad are thankful to Prince Sultan University for paying the APC and support through TAS research lab.

## Funding

No funding source exists.

## References

[1] Christiani David C. Smoking and the molecular epidemiology of lung cancer. Clin Chest Med 2000;21(1):87–93.
[2] Doll Richard, Bradford Hill A. Smoking and carcinoma of the lung, preliminary report, 1950. Bull World Health Organ 1999;77(1):84.
[3] Wynder Ernest L, Graham Evarts A. Tobacco smoking as a possible etiologic factor in bronchiogenic carcinoma: a study of six hundred and eighty-four proved cases. JAMA 1950;143(4):329–36.
[4] Bayne-Jones Stanhope. Smoking and health: report of the advisory committee to the surgeon general of the public health service. No. 1103. US Department of Health, Education, and Welfare, Public Health Service; 1964.
[5] Walser Tonya, et al. Smoking and lung cancer: the role of inflammation. Proc Am Thorac Soc 2008;5(8):811–5.
[6] World Health Organization. Tobacco or health: a global status report. World Health Organization; 1997.
[7] Youlden Danny R, Cramb Susanna M, Baade Peter D. The international epidemiology of lung cancer: geographical distribution and secular trends. J Thorac Oncol 2008;3(8):819–31.
[8] Sasco AJ, Secretan MB, Straif K. Tobacco smoking and cancer: a brief review of recent epidemiological evidence. Lung Cancer 2004;45:S3–9.
[9] Doll R, Peto R, Boreham J, Sutherland I. Mortality in relation to smoking: 50 years' observations on male british doctors. BMJ 2004;328(7455):1519.
[10] Rogot E, Murray JL. Smoking and causes of death among US veterans: 16 years of observation. Public Health Rep 1980;95(3):213.
[11] Proctor Robert N. Tobacco and the global lung cancer epidemic. Nat Rev Cancer 2001;1(1):82–6.
[12] Woloshin Steven, Schwartz Lisa M, Welch Gilbert. The risk of death by age, sex, and smoking status in the United States: putting health risks in context. J Natl Cancer Inst 2008;100(12):845–53.
[13] Weitzman Sigmund A, Gordon Leo I. Inflammation and cancer: role of phagocyte-generated oxidants in carcinogenesis. Blood 1990;76(4):655–63.
[14] Engels Eric A. Inflammation in the development of lung cancer: epidemiological evidence. Expert Rev Anticancer Ther 2008;8(4):605–15.
[15] Fowler AC, Fowler AC. Mathematical models in the applied sciences (Vol. 17). Cambridge University Press; 1997.
[16] Tang TQ, Jan R, Bonyah E, Shah Z, Alzahrani E. Qualitative analysis of the transmission dynamics of dengue with the effect of memory, reinfection, and vaccination. Comput Math Methods Med 2022;2022:20.
[17] Din A, Li Y, Khan T, Zaman G. Mathematical analysis of spread and control of the novel corona virus (COVID-19) in China. Chaos Solitons Fractals 2020;141:110286.
[18] Din A. The stochastic bifurcation analysis and stochastic delayed optimal control for epidemic model with general incidence function. Chaos 2021;31(12):123101.
[19] Farhan M, Shah Z, Jan R, Islam S. A fractional modeling approach of Buruli ulcer in Possum mammals. Phys Scr 2023;98(6):065219.
[20] Alshehri A, Shah Z, Jan R. Mathematical study of the dynamics of lymphatic filariasis infection via fractional-calculus. Eur Phys J Plus 2023;138(3):1–15.
[21] Shah Z, Bonyah E, Alzahrani E, Jan R, Aedh Alreshidi N. Chaotic phenomena and oscillations in dynamical behaviour of financial system via fractional calculus. Complexity 2022;2022:14.
[22] Shah Z, Jan R, Kumam P, Deebani W, Shutaywi M. Fractional dynamics of HIV with source term for the supply of new $CD4+$ T-cells depending on the viral load via Caputo–Fabrizio derivative. Molecules 2021;26(6):1806.
[23] Tang TQ, Shah Z, Jan R, Alzahrani E. Modeling the dynamics of tumor–immune cells interactions via fractional calculus. Eur Phys J Plus 2022;137(3):367.

[24] Din A, Li Y, Khan FM, Khan ZU, Liu P. On analysis of fractional order mathematical model of Hepatitis B using Atangana–Baleanu Caputo (ABC) derivative. Fractals 2022;30(01):2240017.
[25] Din A, Li Y, Yusuf A, Ali AI. Caputo type fractional operator applied to Hepatitis B system. Fractals 2022;30(01):2240023.
[26] Ahmad S, Shah K, Abdeljawad T, Abdalla B. On the approximation of fractal-fractional differential equations using numerical inverse Laplace transform methods. CMES-Comput Model Eng Sci 2023;135(3):2743–65.
[27] Atangana A, Baleanu D. New fractional derivatives with nonlocal and non-singular kernel: theory and application to heat transfer model. 2016, arXiv preprint arXiv: 1602.03408.
[28] Caputo M, Fabrizio M. On the notion of fractional derivative and applications to the hysteresis phenomena. Meccanica 2017;52(13):3043–52.
[29] Caputo M. Linear models of dissipation whose q is almost frequency independent–II. Geophys J Int 1967;13(5):529–39.
[30] Atangana A. Mathematical model of survival of fractional calculus, critics and their impact: How singular is our world? Adv Difference Equ 2021;2021(1):1–59.
[31] Alessandro Abate, Tiwari Ashish, Sastry Shankar. Box invariance in biologically-inspired dynamical systems. Automatica 2009;45(7):1601–10.
[32] Ngungu M, Addai E, Adeniji A, Adam UM, Oshinubi K. Mathematical epidemiological modeling and analysis of monkeypox dynamism with nonpharmaceutical intervention using real data from United Kingdom. Front Public Health 2023;11:1101436.
[33] Shah K, Abdeljawad T, Jarad F, Al-Mdallal Q. On nonlinear conformable fractional order dynamical system via differential transform method. CMES-Comput Model Eng Sci 2023;136(2):1457–72.
[34] Dalir M, Bashour M. Applications of fractional calculus. Appl Math Sci 2010;4(21):1021–32.
[35] Hilfer Rudolf. Applications of fractional calculus in physics. World scientific; 2000.
[36] Magin RL. Fractional calculus models of complex dynamics in biological tissues. Comput Math Appl 2010;59(5):1586–93.
[37] Baba IA, Humphries UW, Rihan FA. Role of vaccines in controlling the spread of COVID-19: A fractional-order model. Vaccines 2023;11(1):145.
[38] Wang Y, Zhao G. A comparative study of fractional-order models for lithium-ion batteries using runge kutta optimizer and electrochemical impedance spectroscopy. Control Eng Pract 2023;133:105451.
[39] Zheng Z, Cai Z, Su G, Huang S, Wang W, Zhang Q, Wang Y. A new fractional-order model for time-dependent damage of rock under true triaxial stresses. Int J Damage Mech 2023;32(1):50–72.
[40] Jeelani MB, Alnahdi AS, Abdo MS, Almalahi MA, Alharthi NH, Shah K. A generalized fractional order model for COV-2 with vaccination effect using real data. Fractals 2023;31(2):2340042.
[41] Ahmad SW, Sarwar M, Shah K, Ahmadian A, Salahshour S. Fractional order mathematical modeling of novel corona virus (COVID-19). Math Methods Appl Sci 2023;46(7):7847–60.
[42] Sinan M, Ansari KJ, Kanwal A, Shah K, Abdeljawad T, Abdalla B. Analysis of the mathematical model of cutaneous leishmaniasis disease. Alex Eng J 2023;72:117–34.
[43] Shah K, Arfan M, Ullah A, Al-Mdallal Q, Ansari KJ, Abdeljawad T. Computational study on the dynamics of fractional order differential equations with applications. Chaos Solitons Fractals 2022;157:111955.
[44] Sinan M, Shah K, Kumam P, Mahariq I, Ansari KJ, Ahmad Z, Shah Z. Fractional order mathematical modeling of typhoid fever disease. Results Phys 2022;32:105044.
[45] Kilbas AA, Srivastava HM, Trujillo JJ. Theory and applications of fractional differential equations (Vol. 204). Amester Dam: Elsevier; 2006.
[46] Khalil R, Horani MA, Yousef A, Sababheh M. A new definition of fractional derivative. J Comput Appl Math 2014;264:65–70.
[47] Roberts Mick G, Heesterbeek JAP. Characterizing the next-generation matrix and basic reproduction number in ecological epidemiology. J Math Biol 2013;66(4):1045–64.
[48] Biggerstaff Matthew, et al. Estimates of the reproduction number for seasonal, pandemic, and zoonotic influenza: a systematic review of the literature. BMC Infect Dis 2014;14(1):1–20.
[49] Chowell Gerardo, Nishiura Hiroshi, Bettencourt LuisMA. Comparative estimation of the reproduction number for pandemic influenza from daily case notification data. J R Soc Interface 2007;4(12):155–66.
[50] Descary Marie-Hêlêne, Froda Sorana. Estimating the basic reproduction number from noisy daily data. J Theoret Biol 2022;2022:111210.
[51] Ma Junling. Estimating epidemic exponential growth rate and basic reproduction number. Infect Dis Model 2020;5:129–41.
[52] Alimohamadi Yousef, Taghdir Maryam, Sepandi Mojtaba. Estimate of the basic reproduction number for COVID-19: a systematic review and meta-analysis. J Prev Med Public Health 2020;53(3):151.
[53] Atangana Abdon, Araz SedaIgret. Advanced analysis in epidemiological modeling: Detection of wave. MedRxiv 2021.
[54] Hsu Sze-Bi. A survey of constructing Lyapunov functions for mathematical models in population biology. Taiwanese J Math 2005;2005:151–73.
[55] Magal P, McCluskey CC, Webb GF. Lyapunov functional and global asymptotic stability for an infection-age model. Appl Anal 2010;89(7):1109–40.
[56] Aponin YM, Aponina EA. The invariance principle of la-salle and mathematical models for the evolution of microbial populations. Comput Res Model 2011;3(2):177–90.